Mar Syst Ocean Technol (2017) 12:80–92
DOI 10.1007/s40868-017-0025-3

Shuttle tanker fuel consumption numerical analysis for improving ship efficiency

Rodrigo Achilles Schiller[1] · Felipe Ruggeri[1,2] · Kazuo Nishimoto[1] · Claudio Mueller Prado Sampaio[1] · Reynaldo Pires da Fonseca[3]

Received: 7 April 2015 / Accepted: 21 March 2017 / Published online: 19 April 2017

Abstract The fuel consumption analysis of a Suezmax tanker customized to the offloading operation in the brazilian coast is performed in order to verify the possible savings produced by the so-called "slow steaming" technique during navigation. This ship is equipped of a single engine/propeller but there is a trend of building new vessels considering an equivalent two engines–two propellers for better safety during navigation and offloading operations, therefore a comparison regarding the propulsive efficiency, fuel consumption, and operational conditions (max engine power, rotation, and cavitation limitations) is performed in order to verify the benefits of this new concept. The methodology applied is based on a mixed approach considering numerical simulations using CFD (computational fluid dynamics) and regression models available in the literature: the first one applied to compute the ship resistance and nominal wake fraction in the propeller plane and the second one applied for the propulsive efficiency prediction, as the propeller curves based on Wageningen B-series. The specific fuel oil consumption curves were obtained from the engine manufacturer catalogue.

Keywords Slow steaming · Fuel consumption · Suezmax tanker · Propulsive efficiency · Operational engine region

✉ Rodrigo Achilles Schiller
digao.schiller@gmail.com

Felipe Ruggeri
ruggeri@argonautica.com.br

[1] University of São Paulo, Av. Professor Mello Moraes, 2231 - Vila Universitaria, São Paulo, SP 05508-030, Brazil

[2] Argonautica Engenharia e Pesquisas, São Paulo, Brazil

[3] CENPES - Petrobrás, Rio de Janeiro, Brazil

List of symbols

c	Specific fuel consumption (g/kWh)
c_{prop}	Propulsive coefficient
g	Gravity acceleration (m/s^2)
hc	Water column of the studied point (m)
hv	Distance from the propeller axis until waterline (m)
k	Form coefficient
ks	Surface rugosity (150×10^{-6} m)
n	Propeller rotation (rps)
w_m	Nominal wake in model scale
w_R	Effect of the rudder(s) on the wake fraction
w_S	Ship nominal wake
t	Thrust deduction factor
A_0	Propeller disk area
A_e	Expanded area
A_P	Projected area
B	Beam
C_A	Allowance coefficient
C_B	Block coefficient
C_F	Friccional coefficient
C_{FS}	Ship friccional coefficient
C_{FM}	Model friccional coefficient
Cons	Daily fuel consumption
C_P	Prismatic coefficient
C_{TS}	Total resistance coefficient
C_{VS}	Viscous resistance coefficient
D	Propeller diameter
KQ_{10}	Torque coefficient
KT_{hull}	Hull thrust coefficient
KT_{prop}	Propeller thrust coefficient
L_{WL}	Waterline length
J	Advance coefficient
MR	Margin for sea conditions

N_{RPM}	Propeller/engine rotations per minute
P	pitch
P_{atm}	Atmospheric pressure
P_{ref}	Water vapor pressure
PM	Engine power
P_0	Hydrostatic pressure
P_1	Pressure in the point closest to the free surface
Q	Torque
R	Propeller radius
R_n	Reynolds number
R_T	Total resistance
S	Wetted area
T	Ship draft
T_h	Thrust
V	Velocity
V_0	Velocity of the incident flow
Z	Number of blades
β_{TA}	Thrust deduction factor due to ventilation
η	Propeller efficiency
η_h	Hull efficiency
η_r	Relative rotative efficiency
η_s	Shaft efficiency
ρ	Water density
ΔC_F	Roughness allowance coefficient
σ	Cavitation index
τ	Loading coefficient

1 Introduction

The heavy fuel oil (HFO) is the most common fuel used in large vessels, as tanker, containerships, and bulk carriers. This fuel is a fraction of the petroleum distillation process and has a high viscosity requiring pre-heating before injection in the engine. This fuel contains a significant amount of particulate and foulness providing pollutants as SO_2, NO_X, and VOC,[1] which can create diseases to the human health. According to [1], more than 900,000 ton of particulate per year is emitted by ships, which corresponds to half of the amount emitted by the car fleet worldwide and about 3% of total human CO_2 emissions. In order to reduce the pollution produced by ships, the IMO[2] defined that vessels should improve their efficiencies and reduce the pollutants emissions.

The IMO introduced the EEDI[3] in the VI annex of MARPOL (International Convention for the Prevention of Pollution from Ships) [2, 3], defining the efficiency levels required for new ships according to the vessel size, type (car carrier, containership, bulk carrier, tanker etc). The index allows the shipowner to choose among the several technologies available in the market since the only requirement is that the emission level is achieved. The first stage requires about 10% of reduction regarding CO_2 emissions for ships built between 2015 and 2020, assuming a reference line defined based on regression studies performed with vessels built from 1999 to 2009. The CO_2 emission reduction shall reach 30% by 2025–2030 for almost the entire fleet.

The regulation also defines the so called SEEMP[4] that should be developed for each ship according to its characteristics containing a collection of "actions" during operation to improve the ship efficiency, for instance, real time routing, speed/ballast/trim optimization, time between maintenance etc.

The main goal of the SEEMP is to define actions for continuous improvements of the ship energy management, which shall be measured by the shipowner using the so-called EEOI.[5] The better ship efficiency may also be verified by the reduction in fuel consumption, therefore, operational costs reduction. The EEOI works as a feedback measurement to verify the effectiveness of SEEMP providing data to verify problems, for instance, engine, hull, propeller, etc, which could be used as predictive method for maintenance.

This study is focused in a shuttle tanker converted from a conventional tanker to perform offloading operations in Santos Basin of Brazil coast. The main goal is to study the fuel consumption reduction due to speed reduction (slow steaming) in order to obtain the order of magnitude in terms of saving if a routing strategy is assumed in the operation. Since a shuttle tanker carries oil from Santos Basin to Brazil ports, half the voyage time the vessel is in ballast; therefore several loading conditions were evaluated to define the optimum ballast to be carried, which will be summarized in practical guides for the operation.

The offshore oil production in Brazil has increased in the last years, therefore new vessels will be required to perform the oil cargo transportation. In order to provide support for the new designs customized for Brazil operation, a comparison of fuel consumption is performed between mono and twin propeller concepts. The brazilian fleet has already started to be renewed through governmental programs such as PROMEF and PAC2, which must follow new IMO rules.

The operational profile defines the shipowner requirements and the optimum operational condition (less fuel consumption). The time distribution of a shuttle tanker with a short course is combined by: voyage time, loading (offloading operation), unloading in the port, and anchored waiting in the anchorages areas close to the port.

[1] Volatile Organic Composites.

[2] International Maritime Organization.

[3] Energy Efficiency Design Index.

[4] Ship Energy Efficiency Management Plan.

[5] Energy Efficiency Operational Index.

The first important aspect is the voyage distance since the oil platforms are located near the coast (less than 150 miles) compared to long course ships. The second important consideration is the high traffic of vessels in brazilian ports, which increases the waiting time in the anchorage regions, exceeding 2 days for most of the ports. The offloading operation requires favorable weather conditions to avoid risk of collision or oil spill so if the weather forecast is provided the vessel can reduce its speed and reduce the fuel consumption. The same situation is verified for the ports owned by the shipowner because the time windows can be adjusted according to the queue length to reduce the waiting time. Under these conditions, the ship speed can be reduced without losses to the operation.

It should be noticed that the effectiveness of these solutions goes beyond the vessel including the logistic planning concerning the port and platform operations that should maintain continuous communication.

2 Methodology

2.1 Numerical models

The vessel studied is a converted tanker to perform offloading operations, therefore this ship has a controllable pitch propeller to provide station keeping assistance during DP[6] mode. The DP system works to maintain the vessel on a reference distance from the oil platform to avoid collisions.

However, due to construction limitations, the controllable pitch propeller has only 7.2 m against 8.6 m fixed pitch propeller previous to the conversion and since the efficiency is proportional to the propeller diameter, it reduces the propulsion efficiency appreciably during navigation, requiring additional power from the main engine. Based on that a new vessel has been studied considering two propellers instead of a single one in order to improve both propulsion efficiency and redundance, the last one important in terms of operational safety.

The ship resistance was computed using a CFD model through StarCCM+ FVM[7] to solve the flow around the hull and compute both ship resistance and nominal wake. The solution in real scale is still a challenge from the numerical point of view due to the high Reynolds, since the boundary layer is proportionally smaller compared to the model scale, requiring a refined mesh to capture the physical phenomena involved. Moreover, the convergence rate is slower requiring more computation resources to solve the flow completely.

[6] Dynamic Positioning.

[7] Finite Volume Methods.

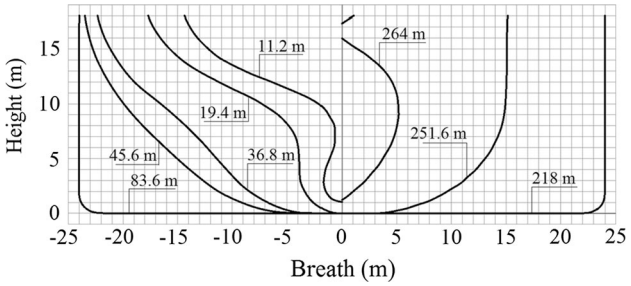

Fig. 1 Line plans of the studied shuttle tanker from the aft perpendicular

In order to reduce the computational resources available, the analyses were performed in a 1:70 scale. The numerical model was built assuming the bare hull, without any kind of appendages. The lines plan is shown in Fig. 1 with some details regarding the fore and stern regions shown in Fig. 2, with the main dimensions summarized in Table 1.

The numerical simulation was performed neglecting free surface effects, since for low speeds the viscous resistance is more important, which was computed using a simplified model by a double body model to avoid the complexity in modeling the free surface using VOF[8] approach. Since the analysis performed required the computation of a considerable amount of simulations, the free surface was neglected to turn the study feasible. The results obtained by the CFD were both ship resistance and the nominal wake (w_S) in the propeller plane.

The hull–propeller–engine integration is performed to define the operational point and fuel consumption. This computation requires the thrust deduction factor computation (t), which is performed following the regression proposed by [4].

The main engine was defined based on a total power of 19 MW (MCR) according to the similar Suezmax ships and according to low rate engines manual presented by MAN Diesel manufacturer catalogue. This is a basic assumption to define the vessel operational conditions for the several speeds and drafts analyzed.

The vessel configurations studied were the Suezmax tanker previous to the retrofit into a shuttle tanker (fixed pitch propeller diameter of 8.6 m), the same tanker after the conversion (equipped with a controllable pitch propeller of 7.2 m diameter), and a new ship concept with the same dimensions but equipped with a twin propeller engine room (the diameter of each propeller is 7.2 m and the axis are 10 m far from the symmetry plane).

The simulated cases are shown in Fig. 3 for each configuration described previously considering the design draft (15.3 m), two partially loaded drafts (13.0 and 10.0 m), and in ballast condition (8.0 m). The results concerning

[8] Volume of Fluid.

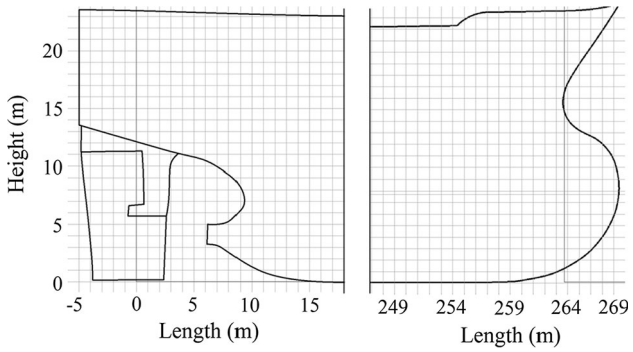

Fig. 2 Fore and stern details of the studied ship

Table 1 Ship dimensions and properties

Parameter	Ship	Model	Units
Length overall	277.3	3.96	m
Length between perp.	264.0	3.77	m
Breadth	48.0	0.69	m
Depth	23.6	0.34	m
Design draft	15.3	0.22	m
Displacement	162207	0.473	ton
Propeller type	Variable pitch		
Propeller diameter	7.2	–	m
Number of blades	4	–	–
Design power	19.0	–	MW
A_e/A_0	0.55	–	–

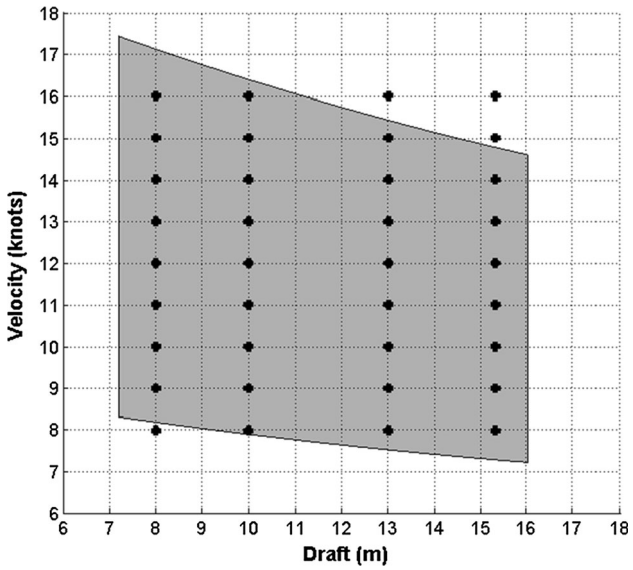

Fig. 3 Ship configurations simulated using the procedure developed (the *gray* zone is the operational region based on the main engine specifications)

other conditions were interpolated among the results. The range of velocities were defined based on the sea trials available for the shuttle tanker (after the retrofit), and the operational zone is highlighted in gray taken into account the maximum power provided by the main engine and the minimum rotation required for a full time operation and the last one provided by engine manual.

2.2 Ship resistance

The ship resistance is evaluated in calm waters (no added resistance considerations were performed) containing two main contributions: viscous and wave resistance, following the traditional approach of Froude. As discussed before, since the speed is small, the viscous resistance (friction and form) achieves almost 90%of the total resistance [4] so the wave resistance is neglected in this initial study.

The viscous resistance is computed by CFD using a double body model (neglecting free surface contribution) and the form factor computed following Prohaska Method for each tested condition [5]. The friccional resistance is estimated based on ITTC-78 correlation line.

In order to compute the total resistance and perform the hull–propeller-integration process, the wave resistance was assumed as 10% of the viscous resistance 3. It should be noticed that the simulations are performed under a typical towing tank scale (1:70) so there is some uncertainties concerning the extrapolation of the form factor to real scale results, since ITTC assumes this factor as constant although there is some numerical observations that it can change with the simulated scale [6, 7].

The typical shuttle tanker sails with different drafts since which can be segregated in three most probable: full loaded from platform to port, partial loaded from platform to port and ballast condition from port to platform. The studied vessel has a 15.3 m design draft, which can be extended to a maximum condition of 16.0 m. The lowest draft considered for navigation was 8.0 m under even keel condition, with the propeller fully submerged to avoid cavitation/ventilation.

The ship resistance in calm water conditions for a clean hull can be calculated following Eq. (1):

$$R_T = C_{TS}\left(\frac{1}{2}\rho V^2 S\right) \tag{1}$$

The viscous resistance coefficient can be computed following the expression discussed before using Eq. (2) and assuming the simplification discussed before the total coefficient is computed based on (3) [8, 9].

$$C_{VS} = (1+k)C_F + \Delta C_F + C_A \tag{2}$$

$$C_{TS} = 1.1 C_{VS} \tag{3}$$

The components $(1+k)C_F$, ΔC_F C_A are the viscous components with k as the form factor and C_F the friccional coefficient computed by (4).

$$C_F = \frac{0.075}{(\log_{10}(R_n) - 2)^2} \tag{4}$$

The components ΔC_F and C_A are used to convert the roughness of the model scale to full scale condition, computed by (5) and (6), respectively.

$$\Delta C_F = 0.044\left[\left(\frac{k_S}{L_{WL}}\right)^{1/3} - 10R_n^{1/3}\right] + 0.000125 \tag{5}$$

$$C_A = (5.68 - 0.6\log_{10}(R_n)) \cdot 10^{-3} \tag{6}$$

2.3 Hull–propeller integration

The propeller characteristic curves were obtained by B-Troost systematic series [10, 11]. The results concerning the characteristics curves can be obtained by the several pitch/diameter ratios, which is important for the controllable pitch configuration. The main characteristics required to obtain the propeller curves are the diameter (D), number of blades (Z), expanded area over the project one, assumed as equal for the three configurations studied. The pitch for the controllable configurations were evaluated in the range $0.6 < P/D < 1.4$. The characteristics concerning the propellers are shown in Table 2.

The results concerning the propeller curves are obtained in open water conditions, without any hull influence, which should be corrected to take into account the hull interaction. In this work, two different phenomena are evaluated: the wake generated by the hull in the propeller and the increase in ship resistance due to the acceleration of flow velocity due to propeller action, which reduces the pressure in the stern region.

The mean nominal wake is evaluated based on the velocity field computed by the CFD simulations using Eq. (7), where r_{hub} is the hub radius, R the propeller radius, and $w(r,\theta)$ the nominal wake computed for each point of the propeller plane defined in cylindrical coordinates.

$$w = \frac{1}{\pi(R - r_{hub})^2}\int_{r_{hub}}^{R}\int_0^{2\pi} w(r,\theta)\,r\,d\theta\,dr \tag{7}$$

Table 2 Propeller characteristics

Number of blades	4
A_e/A_0	0.55
Diameter—fixed pitch (m)	8.6
P / D—fixed pitch	0.8
Diameter—controllable pitch (m)	7.2
P / D—controllable pitch	0.6–1.4

The nominal wake was converted from model scale to real scale based on Eq. (8) [9]. The velocity field and nominal wake is shown in Fig. 4 for the 15.3 m draft condition.

$$w_S = (t - w_R) + (w_M - t - w_R)\frac{(1+k)C_{FS} + \Delta C_F}{(1+k)C_{FM}} \tag{8}$$

The nominal wake fraction was computed based on the velocity field computed in the propeller position using StarCCM+. The computations were performed in model scale in order to simplify the convergence tests and reduce the mesh size. The ITTC-1978 correction methodology was applied in order to obtain estimative of the wake factor in real scale. The standard value assumed by ITTC is 0.04 for w_r. The variations in the velocity field due to the different propeller positions and diameters are noticed, for instance, Fig. 5 shows the differences considering the single and twin propeller conditions ($D = 7.2$ m).

The thrust deduction factors are computed based on [12] following Eqs. (9) and (10) for the mono and twin propeller conditions, respectively.

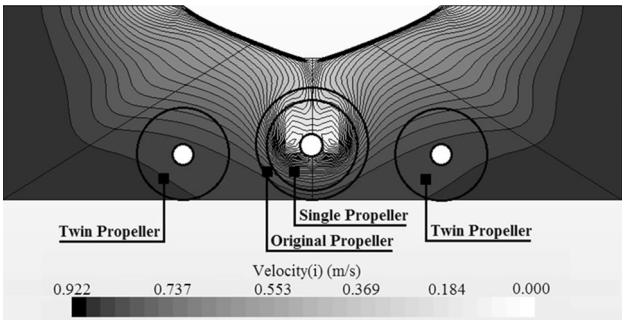

Fig. 4 Axial velocity field in the propeller planes for the original FPP, single CPP, and twin CPP configuration computed using StarCCM+ CFD model

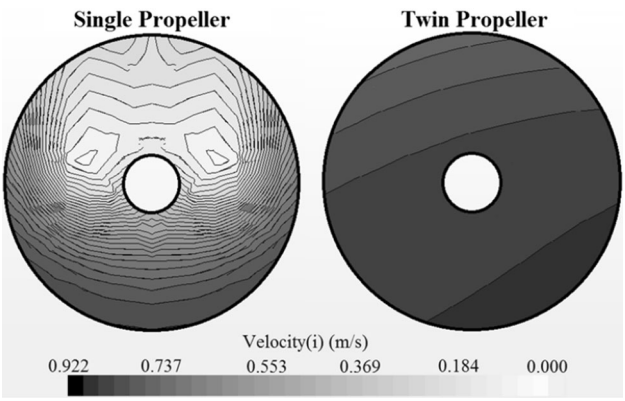

Fig. 5 Comparison between the axial velocity field computed by StarCCM+ simulations for both the single and twin propeller configurations for $D = 7.2$ m

Table 3 Nominal wake (ω_m) and form factor (k) computed by the CFD simulations in model scale, as the wake in real scale based on ITTC formulation and thrust deduction factor (t) computed based on [13] regression

T (m)	$1 \times D = 8.6$ m			$1 \times D = 7.2$ m			$2 \times D = 7.2$ m			k
	w_m	w_s	t	w_m	w_s	t	w_m	w_s	t	
15.3	0.517	0.416	0.239	0.736	0.527	0.244	0.127	0.215	0.222	0.173
13.0	0.485	0.399	0.231	0.710	0.512	0.237	0.121	0.207	0.213	0.166
10.0	0.447	0.369	0.220	0.651	0.479	0.227	0.115	0.196	0.198	0.151
8.0	0.391	0.339	0.210	0.605	0.453	0.220	0.112	0.188	0.187	0.121

$$t = 0.001979\frac{L_{WL}}{B(1-C_P)} + 1.0585\frac{B}{L_{WL}} - 0.00524 - 0.1418\frac{D^2}{BT} \quad (9)$$

$$t = 0.325 \cdot C_B - 0.1885\frac{D}{\sqrt{B \cdot T}} \quad (10)$$

The results concerning the nominal wake and the form factor computed using the CFD simulations are summarized in Table 3 (including the ITTC-1978 real scale correction), as the thrust deduction factor based on the regression.

2.4 Operation point

The operation point is calculated by the advance coefficient equivalence between hull and propeller, which is performed solving Eq. (11) by Newton's method, where $\mathrm{KT_{hull}}(J)$ is evaluated based on (12) and the propeller curve obtained from B-Troost systematic series.

$$f(J) = \mathrm{KT_{hull}}(J) - \mathrm{KT_{prop}}(J) \quad (11)$$

The ship resistance is computed taking into account the added resistance and fouling around the hull combined in the single factor MR = 0.15, according to [14].

$$\mathrm{KT_{hull}} = \frac{R_T \cdot (1 + \mathrm{MR})}{(1-t)\rho D^2 V^2 (1-w_s)^2} J^2 \quad (12)$$

After the advance coefficient is computed the propeller rotation N_{RPM}, propeller thrust T_h and torque Q are obtained by Eqs. (13), (14) and (15).

$$N_{RPM} = \frac{60V(1-w)}{D \cdot J} \quad (13)$$

$$Th = \frac{\mathrm{KT_{prop}}\rho\left(\frac{N_{RPM}}{60}\right)^2 D^4}{\beta_{TA}} \quad (14)$$

$$Q = \frac{KQ_{10}}{10}\rho\left(\frac{N_{RPM}}{60}\right)^2 D^5 \quad (15)$$

The operational points for the several conditions analyzed considering both the mono and twin propeller configurations are shown in Figs. 6 and 7 for the design draft and speed, respectively. The results are presented for several P / D ratios in order to take into account the controllable pitch capability. It can be verified that the maximum propeller efficiency achieved for the single propeller configuration is about 40% for a P / D close to 0.7. On the other hand, the propeller efficiency for the twin propeller configuration is about 60% for a P / D close to 1.

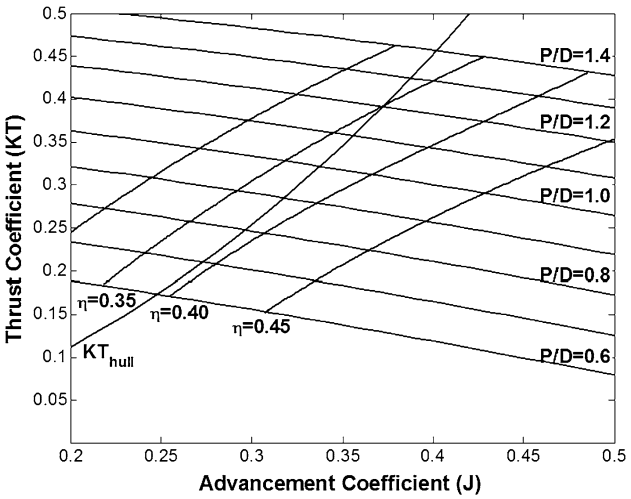

Fig. 6 Thrust coefficient for both hull and propeller assuming several P/D ratios for the single propeller with controllable pitch

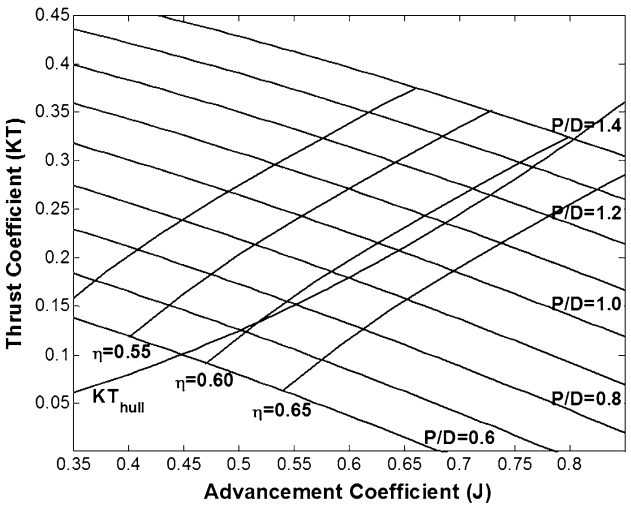

Fig. 7 Thrust coefficient for both hull and propeller assuming several P/D ratios for the double propeller with controllable pitch

2.5 Cavitation and ventilation

Cavitation is the formation of vapor cavities in the water due to the low pressure under constant temperature, which is common for propeller under high load conditions, which can provide excessive noise, vibration, erosion, and reduction of the propulsive power. Since the phenomenon occurs due to pressure drop, the points close to the free surface must be more susceptible compared to the propeller hub due to the hydrostatic pressure variation. The cavitation number is computed following Eq. (16) and for the ratios $(P_0 - P_1)/(\rho V_0^2/2) \geq \sigma$ cavitation should be expected, where V_0 is the incident flow velocity, P_0 is the hydrostatic pressure, and P_1 the pressure in the point closest to the free surface.

$$\sigma = \frac{P_{\text{atm}} + \rho g h c - P_{\text{ref}}}{0.5\rho n^2 D^2 (J^2 + 4.836)} \tag{16}$$

The cavitation is evaluated based on Burril curves [11] for a maximum 5% level, where the factors τ and σ are computed from Eqs. (17) and (18).

$$\tau = \frac{T_{\text{h}}}{0.5\rho A_{\text{p}} V_0^2} \tag{17}$$

$$A_{\text{p}} = \frac{A_{\text{e}}}{A_0}\pi\frac{D^2}{4}\left(1.067 - 0.229\frac{P}{D}\right) \tag{18}$$

The ventilation phenomenon may also occur for propellers close to the free surface under high load condition when the air is drawn into the blades reducing the thrust and torque up to 80%.

The ventilation can be divided in three groups: non-ventilation, partially ventilation, and totally ventilation according to the level of air that is drawn. The thrust reduction is computed using the method proposed by Faltinsen, as described in [15] using Eq. (19), where hv is the vertical distance between the propeller axis and the waterline. A maximum ventilation of 10% was assumed in this work since the propeller would not operate fully submerged anymore above this value.

$$\beta_{\text{TA}} = \begin{cases} 0, & \text{if } \dfrac{\text{hv}}{R} < -0.48 \\ 1, & \text{if } \dfrac{\text{hv}}{R} > 1.3 \\ 1 - 0.675\left(1 - \dfrac{0.769\text{hv}}{R}\right)^{1.258}, & \text{otherwise} \end{cases} \tag{19}$$

The global efficiency is computed following Eq. (20) taken into account the several efficiencies defined previously.

$$c_{\text{prop}} = \eta_{\text{h}}\eta_{\text{r}}\eta_{\text{S}}\eta\beta_{\text{TA}} \tag{20}$$

2.6 Fuel consumption calculation

The fuel consumption is computed based on the hull–propeller integration using the specific fuel oil consumption (SFOC) curves provided by the engine manufacturer selection guide [16, 17]. The engines were selected based on similar vessels. The main characteristics are summarized in Table 4, the 7S70ME-C8.5-TII adopted for the single propeller configuration and the 6S50ME-C9.5-TII for the twin propeller one. The SFOC curves according to the engine load are shown in Fig. 8, where it can be verified the smaller consumption for the second model. The required engine power was computed using Eq. (21) and compared to the engine rotation/power limits in order to verify the feasible of the several combinations of ship draft and speed.

$$\text{PM} = \frac{T_{\text{h}} V (1 - w)}{\eta_{\text{r}}\eta_{\text{S}}\eta} \tag{21}$$

The relative rotative efficiency η_{r} was computed based on the regression model Eqs. (22) and (23) provided by [13] considering the mono and twin propeller configurations, respectively.

$$\eta_{\text{r}} = 0.9922 - 0.05908\frac{A_{\text{e}}}{A_0} + 0.07424(C_{\text{p}} - 0.0225\text{LCB}) \tag{22}$$

Table 4 Main engine properties

Engine type	7S70ME-C8.5-TII	6S50ME-C9.5-TII	Units
SMCR power	19000	9500	kW
SMCR RPM	80/91	115	rpm
Ambient condition	ISO	ISO	–
Reference LVC of fuel oil	42700	42700	kJ/kg
SFOC (SMCR)	168.1	165.2	g/kWh
SFOC (75% of SMCR)	164.2	162.5	g/kWh
SFOC incl. 6% tolerance	174	172.2	g/kWh
	(24% of SMCR)	(26% of SMCR)	

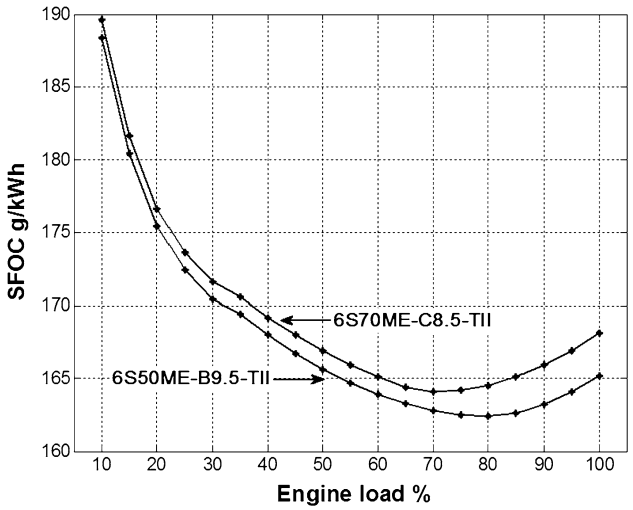

Fig. 8 Specific fuel oil consumption curves for the selected engines based on the manufacturer guideline [16, 17]

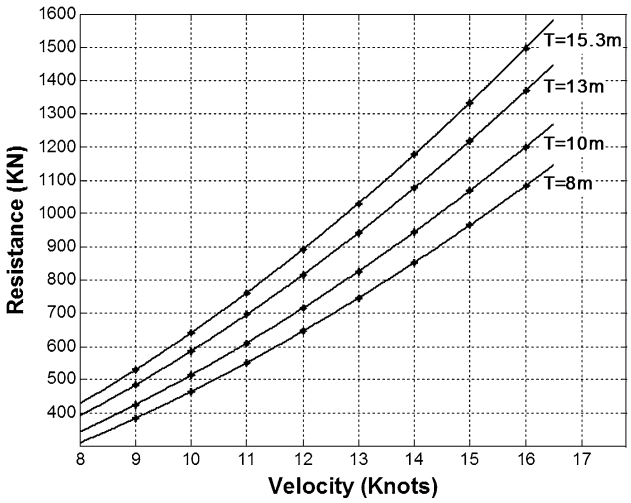

Fig. 9 Ship resistance curves for the bare hull conditions in calm water computed based on the CFD simulation

$$\eta_r = 0.9737 + 0.111(C_p - 0.0225\text{LCB}) - 0.06325\frac{P}{D} \quad (23)$$

The shaft efficiency η_S was assumed as 0.98 for both mono and twin propeller configuration [6, 8]. The specific fuel consumption changes according to the P / D ratio because the engine load condition also changes, therefore the feasible P / D ratio that provides the lowest fuel consumption was considered.

The daily fuel consumption is calculated from Eq. (24), where c is the specific fuel consumption and PM is the engine power.

$$\text{Cons} = 24\frac{c}{10^6}\ \text{PM} \quad (24)$$

3 Results

The ship resistance computed using StarCCM+ was compared to experimental data measured in the IPT Towing Tank considering 4 different speeds and two loading conditions in order to validate the numerical results. The tests were performed for the captive hull condition (not free to trim) in order to provide a better comparison basis with some sand grain strips attached to the model bow to provide a turbulent flow. The comparison is shown in Table 5, where a maximum difference of 6.9% was verified for the maximum speed in ballast condition. It shall be noticed that the free surface was not modeled in the CFD computations thus some differences may be expected. The ship resistance converted to full scale is shown in Fig. 9.

In order to validate the power prediction methodology considering the hull–propeller–engine integration process, the method described earlier was applied to two Suezmax tankers with small differences regarding ship length and beam. The characteristics of the ships, as the predicted power for the maximum speed are shown in Table 6 compared to the informed values. The total power is overpredicted in about 5.8% higher for the first ship and 3.2% for second one, which could be associated with the several approximations performed, for instance, the ship resistance of the studied ship or the sea margins.

Table 5 Comparison between CFD and experiment results regarding ship resistance for the ballast condition ($T_{model} = 0.116$ m – $T_{real} = 8.1$ m) and loaded ($T_{model} = 0.230$ m – $T_{real} = 16.1$ m)

Draft (m)	Speed (m/s)	Ship resistance experimental (N)	Ship resistance CFD (N)	Difference (%)
0.116	0.61	2.42	2.28	5.5
0.116	0.74	3.26	3.09	5.2
0.116	0.86	4.52	4.23	6.4
0.116	0.98	6.09	5.64	6.9
0.230	0.61	3.36	3.18	5.3
0.230	0.74	4.62	4.45	3.6
0.230	0.86	6.19	5.91	4.6
0.230	0.98	7.98	7.49	6.1

Table 6 Similar ship characteristics used for validation

Ship	Da Ming Hu	United dynamic	Units
LOA	275.0	274.0	m
Beam	48.0	50.0	m
Design draft	17.3	17.0	m
Construction year	2003	2010	-
DWT	159149	161653	ton
Eng. manufac.	MANB&W	MANB&W	–
Eng. model	6S70MC	6S70MC	–
Velocity	15.0	15.3	knots
Installed power	16860	18660	kW
Predicted power	17840	19260	kW
Differences	5.8	3.2	%

Table 7 Comparison of the predicted power and propulsive efficiency considering the three propeller–engine configurations for a 14 knots speed

Velocity	14.0 knots		
	$1 \times D = 8.6$ m	$1 \times D = 7.2$ m	$2 \times D = 7.2$ m
η_h	1.303	1.598	0.993
η_r	1.018	1.018	0.991
η_S	0.980	0.980	0.980
η	0.495	0.373	0.624
β_{TA}	1	1	1
c_{prop}	0.643	0.595	0.602
Power	15175 kW	16404 kW	16375 kW
Cons.	59.87 (t/d)	65.08 (t/d)	64.38 (t/d)

The predicted power, fuel consumption, and global efficiency for the three proposed propeller configurations were evaluated for a 14 knots speed under the design draft, achieving the results shown in Table 7.

Since the ship resistance is the fixed, the propulsive coefficient and the engine efficiency are the most important factors related to fuel consumption; the later is a key driver in the analysis since the variations in the specific fuel consumption curve are small. For the design speed of 14 knots and design draft, the original vessel has a propulsive coefficient 6–7% higher than the other propulsive alternatives, while the twin propeller configuration is almost 1% more efficient than the single propeller one. It should be noticed that although the hull and relative rotative efficiencies are smaller in the twin propeller configuration compared to the single one, the propeller efficiency is appreciably higher, providing almost the same propulsive coefficient for this specific condition.

The analysis was extended to the entire operational range of drafts and speeds to verify the advantages concerning each configuration for several operational conditions. The results concerning the power required for each configuration are shown in Fig. 10a–c. The original configuration requires more engine power in the ballast draft compared to the 10 m one due to the loss of efficiency provided by the high ventilation in the propeller, which reduces the thrust and torque appreciably, therefore this navigation conditions was not considered in the study concerning the original vessel.

The efficiency concerning the original vessel is appreciably larger for the 13 m draft compared to the 10 m one. The global efficiency concerning the single propeller configuration is smaller than the twin propeller one for low speeds and the opposite trend is verified for high velocities, thus the best choice may change according to the operational profile.

The fuel consumption comparison concerning the original ship ($D = 8.3$ m), the single propeller configuration ($D = 7.2$ m), and the twin propeller one is shown in Fig. 11 for the several drafts studied. It can be verified that the original configuration is about 5% more economic than the twin propeller one considering the entire operational range and the twin configuration is about 2% more economic than the single propeller one.

The maximum predicted speeds for the several configurations taken into account the 19 MW installed power are summarized in Table 8. It should be noticed that the original configuration loses efficiency drastically for the lowest draft (8.0 m) due to the ventilation. The operational region for each configuration taken into account for the maximum engine power, minimum rotation, maximum draft, and prevention of excessive ventilation is shown in Fig. 12a–c as the gray polygon, which can be optimized by the captain or ship planner according to the ship schedule/operation. In order to provide an idea of the possible economy, some iso-consumption curves are included.

The twin propeller configuration can operate in a large range of drafts and speeds compared to the single propeller solution due to the two engines configuration. This larger operation region has the advantage of providing operational flexibility during short voyages, when the voyage time may be not critical.

In order to verify the possible economies due to the ship speed reduction, the comparison among the several feasible speeds and the maximum one was performed, as summarized in Tables 9 and 10 for the single and twin propeller configurations. It should be noticed that the speed reduction increases voyage time, thus the comparison must be performed in terms of consumption per voyage instead of daily fuel consumption. It can be

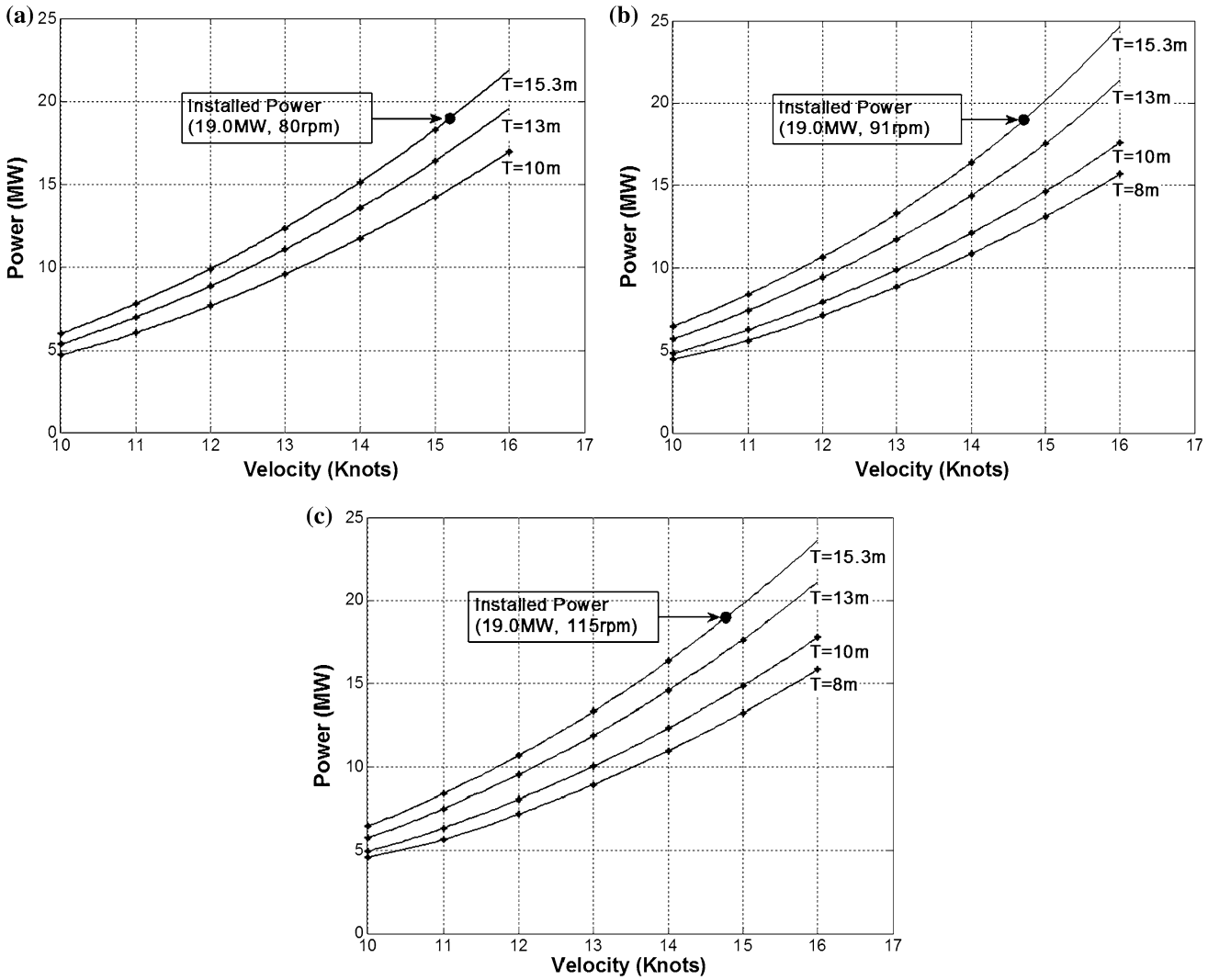

Fig. 10 Power curves for the several propulsive alternatives. **a** Single propeller $D = 8.6$ m, **b** single propeller $D = 7.2$ m and **c** twin propeller $D = 7.2$ m

verified that the fuel consumption reduction per voyage can reach more than 50% by decreasing ship speed to 11 knots for both 15.3 and 10.0 m draft, although the voyage time increases about 40%. Similar results are also verified for both propeller configurations.

It can be verified that even a reduction of 1 knot in ship speed can provide almost 16% fuel consumption decrease per voyage, which is a very effective alternative for the shipowner CO_2 emission policy.

However, previous to implementation of these alternatives, the engine capabilities must be verified since conventional engines may have some problems under low load conditions (below 60% of MCR). According to [18], some of the main problems are:

- Over lubrication of the cylinder lines
- Fouling of the turbochargers and loss of efficiency
- More carbon deposits due to less air flow induced by the turbochargers operating outside the design

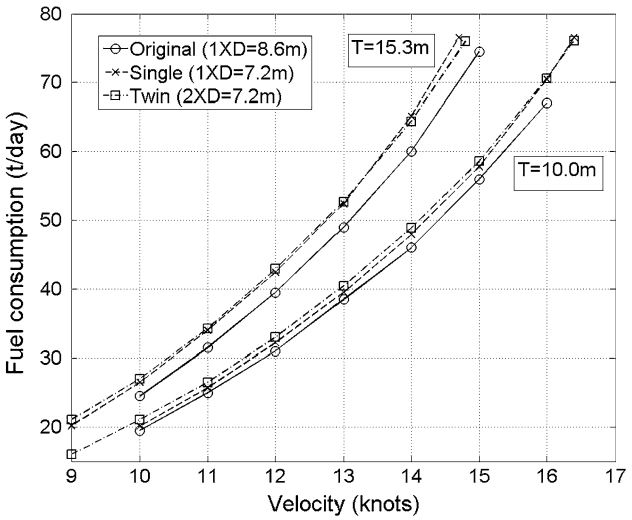

Fig. 11 Comparison of daily fuel consumption among the original configuration ($1 \times D = 8.6$ m), the single propeller ($1 \times D = 7.2$ m) and twin propellers one ($2 \times D = 7.2$ m)

Table 8 Predicted ship speed and fuel consumption at the maximum installed power (19 MW) for the several propeller configurations

	$1 \times D = 8.6$ m		$1 \times D = 7.2$ m		$2 \times D = 7.2$ m	
Draft (m)	Vel (knots)	Fuel cons. (ton/days)	Vel (knots)	Fuel cons. (ton/days)	Vel (knots)	Fuel cons. (ton/days)
15.3	15.2	76.7	14.7	76.5	14.8	76.0
13.0	15.8	76.6	15.4	76.5	15.4	76.1
10.0	16.7	76.6	16.4	76.5	16.4	76.1
08.0	16.1	76.7	17.1	76.7	17.1	75.9

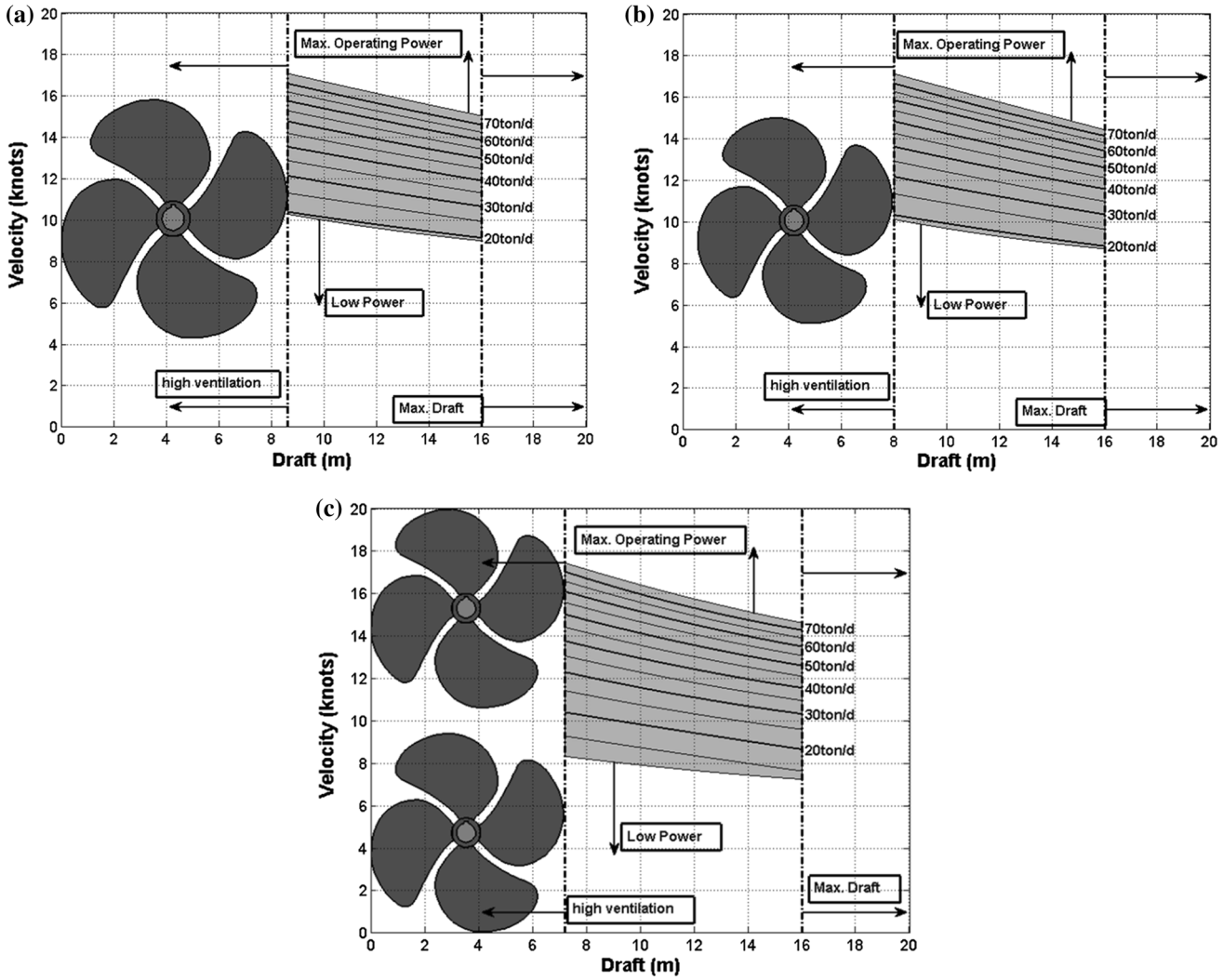

Fig. 12 Operational region for the several propulsive alternatives considering the maximum engine power, minimum engine rotation, excessive ventilation, and maximum draft. **a** Single propeller $D = 7.2$ m, **b** single propeller $D = 8.6$ m, and **c** twin propeller $D = 7.2$ m

range, therefore the maintenance schedule shall be modified

– Damage may occur if engine is run at higher loads after a long period operating in slow steaming

Several new engines and equipments are available for new ships or retrofits to allow slow steaming without damages to the engine [19], although the cost may be prohibitive for a retrofit in some cases due to the complexity involved.

Table 9 Comparison of the daily fuel consumption reduction, fuel consumption reduction per voyage, and increased navigation time per voyage for the single propeller ($1 \times D = 7.2$ m) configuration under 10.0 and 15.3 m draft

	T =10.0 m			T =15.3 m		
Velocity (knots)	Fuel cons. (t/days)	Voyage time increase (%)	Fuel cons. reduction.(%)	Fuel cons. (t/days)	Voyage time increase (%)	Fuel cons. reduction.(%)
16.4	76.5	0.0	0.0	–	–	–
16.0	70.4	2.5	5.6	–	–	–
15.0	57.8	9.3	17.4	–	–	–
14.7	–	–	–	76.5	0.0	0.0
14.0	47.9	17.1	26.7	65.1	5.0	10.7
13.0	39.5	26.2	34.8	52.4	13.1	22.6
12.0	32.2	36.7	42.5	42.4	22.5	32.0
11.0	25.7	49.1	50.0	34.0	33.6	40.7
10.0	20.1	64.0	57.0	26.5	47.0	49.0
9.0	–	–	–	20.2	63.0	56.9

Table 10 Comparison of the daily fuel consumption reduction, fuel consumption reduction per voyage, and increased navigation time per voyage for the twin propeller ($2 \times D$ =7.2 m) configuration under 10.0 and 15.3 m draft

	T =10.0 m			T =15.3 m		
Velocity (knots)	Fuel cons. (t/days)	Voyage time increase (%)	Fuel cons. reduction.(%)	Fuel cons. (t/days)	Voyage time increase (%)	Fuel cons. reduction.(%)
16.4	76.1	0.0	0.0	–	–	–
16.0	70.6	2.5	4.9	–	–	–
15.0	58.6	9.3	15.9	–	–	–
14.8	–	–	–	76.0	0.0	0.0
14.0	48.9	17.1	24.7	64.4	5.7	10.5
13.0	40.5	26.2	32.9	52.7	13.8	21.1
12.0	33.0	36.7	40.7	42.9	23.3	30.4
11.0	26.5	49.1	48.1	34.3	34.5	39.2
10.0	21.1	64.0	54.5	27.0	48.8	47.5
09.0	16.0	82.2	61.6	21.1	64.4	54.3

4 Conclusions

The shuttle tanker was studied to verify the fuel consumption reduction per voyage due to the ship speed reduction (slow steaming), which can reach almost 50% reducing the ship velocity from 16 to 10 knots. The CFD ship resistance model applied for the form factor and wake fraction computation was in fair agreement with the experimental tests performed for both drafts.

The fuel consumption model using the CFD results combined to the regression models and wageningen B-series could provide reasonable predictions of the installed ship power compared to two similar vessels.

The comparison among three concepts of propulsive arrangements was performed considering the original tanker (previous to the conversion into a shuttle tanker) with a 8.6 m propeller diameter (fixed pitch) and the converted vessel with a single controllable pitch propeller with 7.2 m diameter or the twin 7.2 m diameter propeller concept.

The replacement of the original propeller by the controllable pitch one, required for DP operations, reduces the propulsion efficiency about 7%, regardless the assumed pitch. The main conclusions are that both single and twin propeller concepts present almost the same efficiency for the analyzed conditions. However, the operational range concerning both ship speed and draft is larger in the second configuration, providing also redundancy for the DP operation because even with a failure in one engine the other one would still operate.

On the other hand, the twin propeller is more complex in terms of design and construction, therefore it should be more expansive compared to the single propeller solution.

For the new vessels, some important aspects should be taken into account:

– The vessel should be optimized for the operational profile, which can reduce fuel consumption by changing the design speed.

- The application of new low emission engines in order to reduce the amount of CO_2 and particulate.
- Previous to the application of the slow steaming technique, some studies are required to verify the feasibility since there are several adverse effects in the engine.

Acknowledgements The authors would like to thank Petrobras S.A for the financial support provided during this research. The authors gratefully acknowledge the strategic importance of the support given by ANP (Brazil's National Oil, Natural Gas and Biofuels Agency) through the R&D levy regulation.

References

1. D.A. Lack et al., Particulate emissions from commercial shipping: chemical, physical, and optical properties. J. Geophys. Res. **114**(D7), 1–26 (2009). doi:10.1029/2008JD011300
2. DNV, *Marpol 73/78 Annex VI—Regulations for the Prevention of Air Pollution from Ships*. Technical and operational implications (2009), pp. 1–29
3. International Maritime Organisation (IMO), *MARPOL Annex VI and NTC 2008 with Guidelines for Implementation*, 2013 edn. (2013), p. 340
4. L. Larsson, H.C. Raven, in *Ship Resistance and Flow*, ed. By J.R. Paulling. The principles of naval architecture series (The Society of Naval Architects and Marine Engineers, 2010), pp. 17–75
5. C.W. Prohaska, A simple method for evaluation of form factor and the low speed wave resistance. In *Proceedings of the 11th ITTC* (1996), pp. 65–66
6. J.-S. Kouh, Y.-J. Chen, S.-W. Chau, Numerical study on scale effect of form factor. Ocean Eng. **36**(5), 403–413 (2009). doi:10.1016/j.oceaneng.2009.01.011
7. K.-S. Min, S.-H. Kang, Study on the form factor and full-scale ship resistance prediction method. J. Mar. Sci. Technol. **15**(2), 108–118 (2010). doi:10.1007/s00773-009-0077-y
8. International Towing Tank Conference, Recommended procedures and guidelines. In *ITTC Performance Prediction Method, Revision 02* (2011), pp. 1–9
9. International Towing Tank Conference, Final report and recommendations to the 24th itcc. In *Proceedings of the 24th ITTC the Resistance Committee* (2005)
10. S. Ekinci, A practical approach for design of marine propellers with systematic propeller series. Brodogradnja **62**(2), 123 (2011)
11. J. Carlton, in *Marine Propellers and Propulsion*, 3rd edn. (Butterworth-Heinemann, 2012)
12. J. Holtrop, G.G.J. Mennen, An approximate power prediction method. Int. Shipbuild. Prog. **29**, 166–170 (1982)
13. H. Schneekluth, V. Bertram, in *Ship Design for Efficiency and Economy*, 2nd edn. (Butterworth-Heinemann, 1998), p. 224
14. M. Diesel, Turbo propulsion trends in tankers. Mar. Eng. **1**, 1–19 (2009)
15. O.N. Smogeli, in *Control of Marine Propellers: From Normal to Extreme Conditions*. Ph.D. Thesis, Faculty of Engineering Science & Technology, Department of Marine Technology, NTNU (2006), p. 322
16. Man B&W, Man B&W s60me-c8.2-tII—Project Guide—Electronically Controlled Two-stroke Engines, Edition 0.5. (2014), pp. 1–377
17. MAN B&W, Man B&W s50me-c8.2 IMO Tier II—Project Guide—Electronically Controlled Two-stroke Engines, Edition 0.5. (2014), pp. 1–330
18. M. Sanguri, The guide to slow steaming on ships. Mar. Insight **1**, 1–30 (2012)
19. A. Wiesmann, Slow steaming—a viable long-term option? Wärtsilä Tech. J. **2**, 49–55 (2010)